Histochem Cell Biol (2014) 141:75–84
DOI 10.1007/s00418-013-1132-7

ORIGINAL PAPER

Neonatal steroids induce a down-regulation of tenascin-C and elastin and cause a deceleration of the first phase and an acceleration of the second phase of lung alveolarization

Matthias Roth-Kleiner · Thomas M. Berger · Sandrine Gremlich · Stefan A. Tschanz · Sonja I. Mund · Martin Post · Marco Stampanoni · Johannes C. Schittny

Accepted: 24 July 2013 / Published online: 4 August 2013

Abstract Pre- and postnatal corticosteroids are often used in perinatal medicine to improve pulmonary function in preterm infants. To mimic this clinical situation, newborn rats were treated systemically with dexamethasone (Dex), 0.1–0.01 mg/kg/day on days P1–P4. We hypothesized that postnatal Dex may have an impact on alveolarization by interfering with extracellular matrix proteins and cellular differentiation. Morphological alterations were observed on 3D images obtained by high-resolution synchrotron radiation X-ray tomographic microscopy. Alveolarization was quantified stereologically by estimating the formation of new septa between days P4 and P60. The parenchymal expression of tenascin-C (TNC), smooth muscle actin (SMA), and elastin was measured by immunofluorescence and gene expression for TNC by qRT-PCR. After Dex treatment, the first phase of alveolarization was significantly delayed between days P6 and P10, whereas the second phase was accelerated. Elastin and SMA expressions were delayed by Dex treatment, whereas TNC expression was delayed and prolonged. A short course of neonatal steroids impairs the first phase of alveolarization, most likely by altering the TNC and elastin expression. Due to an overshooting catch-up during the second phase of alveolarization, the differences disappear when the animals reach adulthood.

Keywords Tenascin · Elastin · Alveolarization · Smooth muscle actin · Lung development · Steroids

M. Roth-Kleiner (✉) · S. Gremlich
Clinic of Neonatology, University Hospital and University of Lausanne, Avenue Pierre Decker, 1011 Lausanne, Switzerland
e-mail: Matthias.roth@chuv.ch

T. M. Berger
Neonatal and Pediatric Intensive Care Unit, Children's Hospital of Lucerne, 6000 Lucerne 16, Switzerland

S. A. Tschanz · S. I. Mund · J. C. Schittny
Institute of Anatomy, University of Berne, Baltzerstrasse 2, 3012 Bern, Switzerland

M. Post
Physiology and Experimental Medicine Program, Hospital for Sick Children, Toronto, 555 University Avenue, McMaster Building, Room 2006, Toronto ON M5G 1X8, Canada

M. Stampanoni
Paul Scherrer Institute, Villigen, Swiss Light Source, WBBA/216, 5232 Villigen, Switzerland

Introduction

Since Liggins and Howie have shown a beneficial effect on survival of preterm infants after prenatal steroid administration to their mothers, glucocorticoid treatment has become a standard in modern perinatal medicine (Liggins and Howie 1972). Postnatal steroid treatment of ventilated preterm infants has been shown to improve gas exchange, to shorten the duration of ventilator dependency and to reduce the risk of developing chronic lung disease (Doyle et al. 2010). This is explained by a beneficial effect of steroids on surfactant production and secretion, by enhanced perinatal lung fluid clearance, by increased activity of antioxidant enzymes, and by decreased permeability of pulmonary vasculature [for review see (Grier and Halliday 2004)]. Although beneficial effects of postnatal steroids on pulmonary outcome have been proven in clinical studies (Doyle et al. 2010), several animal models raised concerns about their potentially negative impact on lung development. Administration of low-dose dexamethasone (Dex) during 10–14 days beginning as early as

postnatal days 2–4 in rats inhibited alveolarization with a long-lasting effect of reduced lung parenchyma complexity (Blanco et al. 1989; Tschanz et al. 1995). In addition, acute adverse effects of postnatal steroid treatment including gastrointestinal bleeding and perforation, neonatal hypertension and hyperglycemia as well as increasing evidence of a negative impact on long-term outcome (e.g., impaired neurodevelopment, growth restriction, cerebral palsy) have dampened their postnatal use over the last years (Eichenwald and Stark 2007; Halliday 2004). For these reasons, there is a trend in clinical practice to use the lowest effective dose over the shortest possible period (Halliday 2011).

The classic model of alveolarization postulates that a double-layered alveolar capillary network is required for formation of new alveoli and that this process ceases when the alveolar septa have matured by fusion of the microvasculature to a single capillary layer (Burri 2006). Recently, it was shown in various species including humans that alveolarization continues until young adulthood which is far beyond the maturation of the microvasculature (Hyde et al. 2007; Mund et al. 2008; Narayanan et al. 2012; Schittny et al. 2008). Duplication of the capillary network at the base of newly forming alveolar septa permits alveolarization even after maturation of the microvasculature (Schittny et al. 2008). This mechanism was called *late alveolarization*. Due to the fact that classical and late alveolarization may take place in parallel, the phase during which classical alveolarization is predominant is now called *first phase of alveolarization* (postnatal days 4–21 in rats) and the one with dominantly late alveolarization is named *second phase of alveolarization* (day 14—young adulthood). The overlap of the two phases emphasizes that classical alveolar formation blends over in late alveolarization.

In order to mirror the clinical use of neonatal steroids, we analyzed the effect of the administration of a short regimen of Dex to newborn rats for only the first four postnatal days. As shown previously, this resulted in a marked acceleration of lung vascular maturation at the end of the treatment period on P4 (Roth-Kleiner et al. 2005; Tschanz et al. 2003). However, lung development was delayed with a transient loss of parenchymal complexity (Schwyter et al. 2003). To the best of our knowledge, the precise timing of the parenchymal alterations, their correlation to the first and second phase of alveolarization, and the role of extracellular factors have never been studied. Therefore, we (1) studied the formation of new alveolar septa as a measure of alveolarization and (2) analyzed the temporal and spatial expression of tenascin-C (TNC), elastin, and smooth muscle actin (SMA)—three factors involved in alveolarization. Elastin is produced by myofibroblasts at the newly forming free septal edge (septal tip in 2-dimensional lung sections). Elastin and myofibroblasts are required for the formation of new septa (Bostrom et al. 1996, 2002; Lindahl et al. 1997; McGowan et al. 2008). TNC is induced by mechanical stress, contributes to the regulation of cell adhesion, and shows a specific expression pattern during lung development (Chiquet et al. 2004; Yamamoto et al. 1999; Young et al. 1994).

Methods

Animals and tissues

All parts of the animal experiments were approved and supervised by the Swiss Agency for the Environment, Forests and Landscape and the Veterinary Service of the Canton of Bern. Newborn Sprague–Dawley male rat pups were subcutaneously injected with dexamethasone sodium phosphate (Decadron, Merck Sharp & Dohme AG, Glattbrugg, Switzerland) on postnatal days P1–P4 (P1: 0.1 mg, P2: 0.05 mg; P3: 0.025 mg; P4: 0.01 mg per kg body weight) or an equivalent volume of NaCl 0.9 % (controls). For the stereological measurements and the visualization of the tissue, lungs were prepared on postnatal days P4, P6, P10, P21, P36, and P60 according to Schittny et al. (Corroyer et al. 2002; Schittny et al. 1997, 1998). Briefly, after applying a pneumothorax, the lungs were fixed by intratracheal instillation of 4 % paraformaldehyde in phosphate-buffered saline at a constant pressure of 20 cm H_2O water column. The pressure was maintained for at least 4 h. Thereafter, the volumes of the separated lung lobes were measured by water displacement, and the lung volume was calculated (Scherle 1970).

Immunohistochemistry

Tenascin-C (TNC) and SMA double labeling of paraffin sections were done according to routine protocols (Faber et al. 1992; Schittny et al. 1995). Briefly, sections were unmasked with 0.1 % pronase (Roche, Rotkreuz, Switzerland) in PBS and blocked with 5 % BSA (bovine serum albumin) and 1 % newborn goat serum in TRIS-buffered saline (TBS). Mouse anti-alpha-smooth muscle actin (clone 1A4, Sigma-A-2547, Sigma-Aldrich, Buchs, Switzerland) was diluted 1:1,000 in blocking solution and applied at 4 °C over night. Anti-TNC (rabbit anti-chicken, a gift of Matthias Chiquet, Bern) was diluted 1:50 in blocking solution and applied for 1 h at room temperature. Bound antibodies were visualized using Cy3-labeled affinity-isolated goat anti-rabbit IgG (The Jackson Laboratory, Bar Harbor, Maine, USA) and Alexa 488 labeled goat anti-mouse IgG (Molecular Probes, Life Technologies Europe B.V., Zug, Switzerland) diluted 1:1,000 or 1:500,

respectively, in TBS containing 5 % BSA for 1 h at room temperature. Elastin staining was done similarly using rabbit anti-rat elastin (Chemicon AB2039, Millipore, Zug, Switzerland), diluted 1:100 for 1 h at room temperature. Negative controls were performed with non-specific mouse or rabbit IgG (Luyet et al. 2002). None or only little non-specific background was observed in all negative controls. The shown samples were taken from all parts of the lung. No significant differences between central and peripheral regions of the lung were observed under all conditions.

Stereology

Estimations were done according to Schittny et al. (2008). Briefly, the right middle lobes were embedded in paraffin and 10–13 isotropic uniform random step sections were cut perpendicular to the longitudinal axis of the lobe, without special attention to orientation. Sections were stained with hematoxylin and eosin, and 40–60 images were taken systematic randomly (Hsia et al. 2010). The volume density of the lung parenchyma was estimated by point counting. The absolute parenchymal volume was calculated as the product of the parenchymal volume density and the lung volume for each animal and time point (Howard and Reed 2005). As an approximation for alveolarization, septation (the formation of new septa) was assessed by estimating the length of the free septal edge (length of alveolar entrance rings). Based on the growth of the lung (increase in lung volume) during development, we calculated how much of the estimated increase in the length of the free septal edge is caused purely by growth and how much is caused by the formation of new septa (Schittny et al. 2008).

Statistical analysis

For all measurements, 3–5 animals per time point were used. Data were analyzed using one-way analysis of variance (ANOVA) coupled with post hoc Duncan test for multiple pair wise comparisons. Significance level was set at $P < 0.05$.

Synchrotron radiation X-ray tomographic microscopy (SRXTM)

Lung samples, obtained as described above, were embedded in Epon, milled down to a rod of 1.5 mm as described recently (Roth-Kleiner et al. 2005), and scanned by a monochromatic X-ray beam (12.398 keV) at the microtomography station of the Materials Science Beamline at the Swiss Light Source (Paul-Scherrer-Institut, Villigen, Switzerland) (Schittny et al. 2008). The software Imaris (Bitplane AG, Zürich, Switzerland) was used for 3D visualization and surface rendering (Haberthur et al. 2010; Schittny et al. 2008).

TNC gene expression measurements by qRT-PCR

Tenascin-C (TNC) gene expression was measured in lung tissue of treated and untreated animals ($n = 3$–5) on days P4 and P10, as described recently (Trummer-Menzi et al. 2012). Primer sequences for TNC, identified with Primer-BLAST software (National Center for Biotechnology Information; www.ncbi.nlm.nih.gov), are forward: ATG CAC CCA GGG ACT TAC AG and reverse: GCT TGC TCT TAT GTC TGC CC.

Results

Histology

Three-dimensional visualization by SRXTM of untreated rat lungs at postnatal days P4 and P21 (Fig. 1a, c) revealed the known phenotype of the first phase of alveolarization, meaning an overall decrease in size of peripheral gas-exchange units due to subdivision of the large sacculi by newly formed secondary septa. During the second phase of alveolarization between days P14 and P60 (Fig. 1c, e), the formation of new alveolar septa continued, and the complexity of lung parenchyma increased further. While during the first phase, the formation of new septa/alveoli exceeded growth of lung volume, this ratio inversed during the second phase. As a result, the visual impression of the size (diameter) of alveoli decreased between days P4 and P21 and increased again between days P21 and P60 (Fig. 1). In the Dex-treated animals (Fig. 1b, d, f), this process seemed to be disturbed at P4, as there were larger terminal airspaces (Fig. 1b) compared to untreated age-matched controls (Fig. 1a). By day P21, no such difference was recognizable anymore (Fig. 1c, d). Unexpectedly, smaller airspaces were observed in the Dex group on day P36, which indicates an accelerated second phase of alveolarization. On day P60, no difference was observed anymore (Fig. 1e, f).

Morphometry of septal formation

In order to quantify this visual impression of delayed alveolarization, the total length of free septal edges was estimated (Fig. 2b), and the "Anlage" (formation) of new septa as an indicator of the ongoing alveolarization process was calculated (Fig. 2a). As basis for this calculation, we mathematically distinguished between the increase in the free septal edges due to the overall growth of the lung ($\sim$10 % of total increase between days P4 and P60) and

Fig. 1 Synchrotron radiation X-ray tomographic microscopy images of alveoli. 3D images of the terminal ends of the airways of rat lungs between postnatal days P4 to P60 in controls (*panels* **a**, **c**, **e**) and in Dex-treated animals (*panels* **b**, **d**, **f**). *Arrows* point to uplifted new secondary septa, which are very abundant on days P4 and P21

the increase due to the formation of new septa (~90 %). In control animals, the first phase of alveolarization (P4–P21) corresponded to a tremendous increase in the total length of septal edges (Fig. 2b), and a similar increase in newly formed septa from 100 % set at P4 to 516 % length at P21 (Fig. 2a). Thereafter, formation of new septa continued into young adulthood (822 %). During this second phase of alveolarization, an important increase in absolute length of

free septal edges took place (P21: 2,067 m; P60: 4,674 m, Fig. 2b). In Dex-treated rats, the first phase of alveolarization was impaired, manifested as a significantly lower increase in the total length of free septal edges and a less abundant formation of new secondary septa at Dex-P6 (150 %) and Dex-P10 (268 %) compared to CTRL (P6:190 %, $P = 0.04$; P10: 329 %, $P = 0.01$) (Fig. 2). During second phase of alveolarization, however, an inverse trend was measured in lungs of Dex-treated animals with accelerated alveolar formation. Dex induced a statistically significant increase in the total length of the free septal edges and an acceleration of new septal formation at P36 (P36: 638 %, vs. Dex-P36: 781 %, $P = 0.03$; Fig. 2). In young adulthood (P60), this catch-up alveolar formation had stopped with no differences between CTRL and Dex-treated animals, neither in total length of free septal edges nor in the "Anlage" of new secondary septa.

Immunohistochemistry

Knowing the importance of extracellular matrix (ECM) proteins and myofibroblasts in the process of uplifting of new secondary septa, we investigated the time-dependent expression pattern of TNC, elastin, and SMA (as a marker for myofibroblasts) by immunohistochemistry. In controls, TNC was already expressed on P1, typically at the tips of the newly formed septa, corresponding to the entrance ring of the alveoli (Fig. 3a). Its expression almost ceased by P16 (Fig. 3e). SMA showed a strong expression in the same localization, but appeared later (not present on P1 (Fig. 3a), only on P4 (Fig. 3c) and was still present on P16 (Fig. 3e) and adulthood (data not shown). Due to Dex treatment, expression of TNC was delayed by 5 days, appearing not before P6 (Fig. 3b, d); however, its presence was prolonged in Dex-treated animals, still being visible on P16 (Fig. 3f). SMA expression pattern was not markedly changed by Dex (Fig. 3b, d, f).

Elastin fibers in lung tissue could be identified in lung parenchyma of controls already on P1 (not shown). It was rarely but evenly distributed over all of the septal walls on P3 (Fig. 4a) and also in the wall of blood vessels. Its expression strongly increased until P10 with an expression pattern shifting toward the tips of newly formed septa (Fig. 4c, e). In alveolar septa of Dex-treated animals, only small amounts of elastin were observed at P3 (Fig. 4b). By P6, the localization of elastin fibers in Dex-treated animals corresponded more to the phenotype of non-treated controls on P3, with a less important elastin concentration at the septal tips compared to CTRL (Fig. 4c, d). By P10, no difference was observed anymore between CTRL and Dex-treated lungs (Fig. 4e, f).

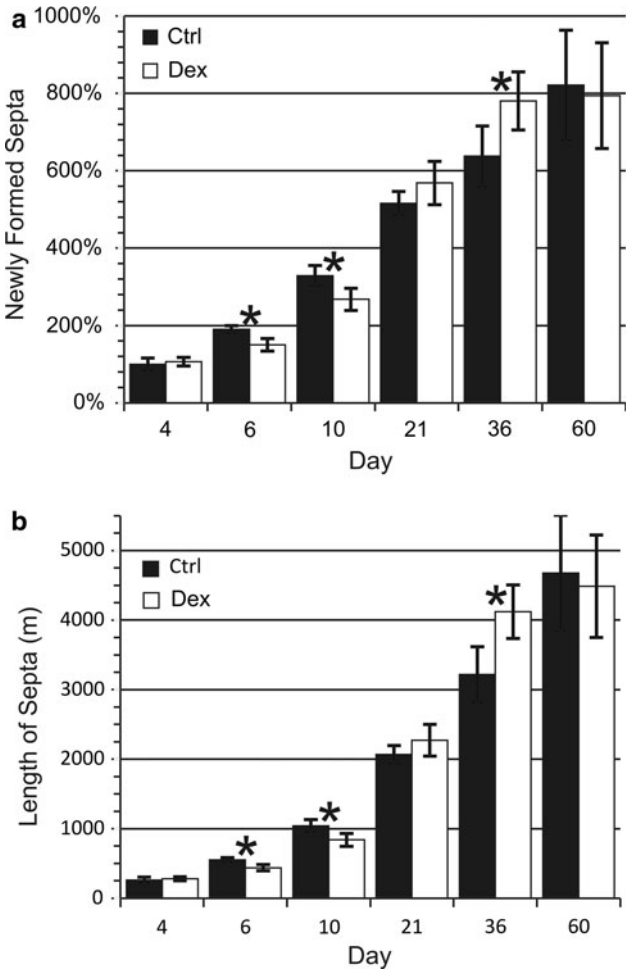

Fig. 2 "Anlage of septa" and length of free septal edges. The "anlage" of newly forming alveolar septa was calculated by mathematically distinguishing between the increase in the length of the free septal edge due to the overall growth of the lung and the increase due to the formation of new alveolar septa. In *panel* **a**, the anlage of new septa is compared between CTRL (*black bars*) and Dex-treated rats (*white bars*). It is expressed as a percentage of the initial length of septa in control animals on postnatal day P4 (=100 %). Only the increase in length due to the formation of new septa is shown. The original data (estimation of total length of septa in meters) are shown in *panel* **b**. *$P < 0.05$ comparing CTRL and Dex of the same day

TNC gene expression

In animals treated with Dex, TNC expression was significantly reduced already by P4 compared to CTRL, but no longer on P10 (Fig. 5).

Discussion

In clinical practice of perinatal medicine, glucocorticoids hold an important place in the prevention and treatment for respiratory insufficiency in preterm infants. Their

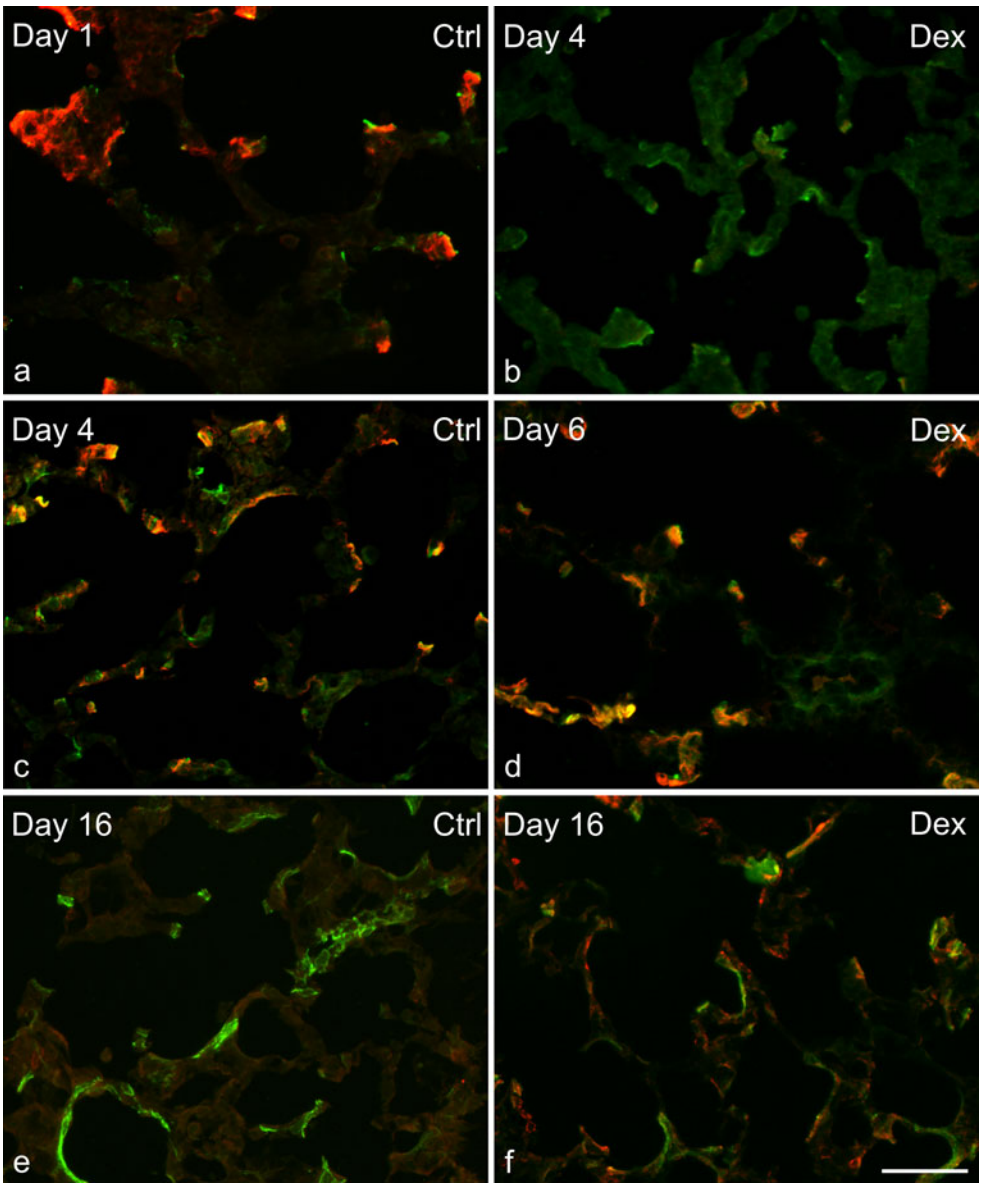

Fig. 3 Co-localization of TNC and SMA. Expression of TNC (*red fluorescence*) and SMA (*green fluorescence*) by immunofluorescence in lung tissue of neonatal rats: in lung parenchyma, TNC and SMA were both expressed at the tips of alveolar septa. In controls (**a**, **c**, **e**), TNC appeared already on postnatal day P1 (**a**). It was detected ~2 days earlier than SMA (**c**). While TNC was down-regulated on P16 (**e**), SMA was still expressed (**e**). In Dex-treated animals, TNC expression was delayed by 5 days, appearing only on P6 (**d**) and prolonged, because small amounts were still observable on P16 (**f**), i.e., 2 days longer than in the controls (**e**). *Bar* 50 μm

beneficial effect on gas exchange by increasing surfactant production and secretion, their anti-inflammatory properties on lung capillaries, and the acceleration of lung liquid absorption are undisputed. However, their impact on lung structure is more controversial (Banks et al. 2002). We demonstrate in this study that already a short regimen of systemic Dex provoked a delay of the start of alveolarization. We were able to show by 3D reconstruction of lung tissue as well as by stereology, that septal formation, aimed at subdividing the sacculi into new alveoli with the goal of increasing gas-exchange surface, was delayed by Dex. By P6 and P10, we found a significant reduction in the complexity of lung structure in Dex-treated animals compared to CTRL. Classical alveolarization, today also called first phase of alveolarization, mainly occurs in rats between P4 and P21 and consists in uplifting of new septal structures at sites where specific ECM proteins and myofibroblasts are accumulated (Schittny et al. 2008). We therefore focused on the effect of Dex on the expression of TNC, elastin, and SMA. In mammals, TNC shows a specific spatial and temporal expression pattern with two peaks during lung development: a first one during airway branching (in rats

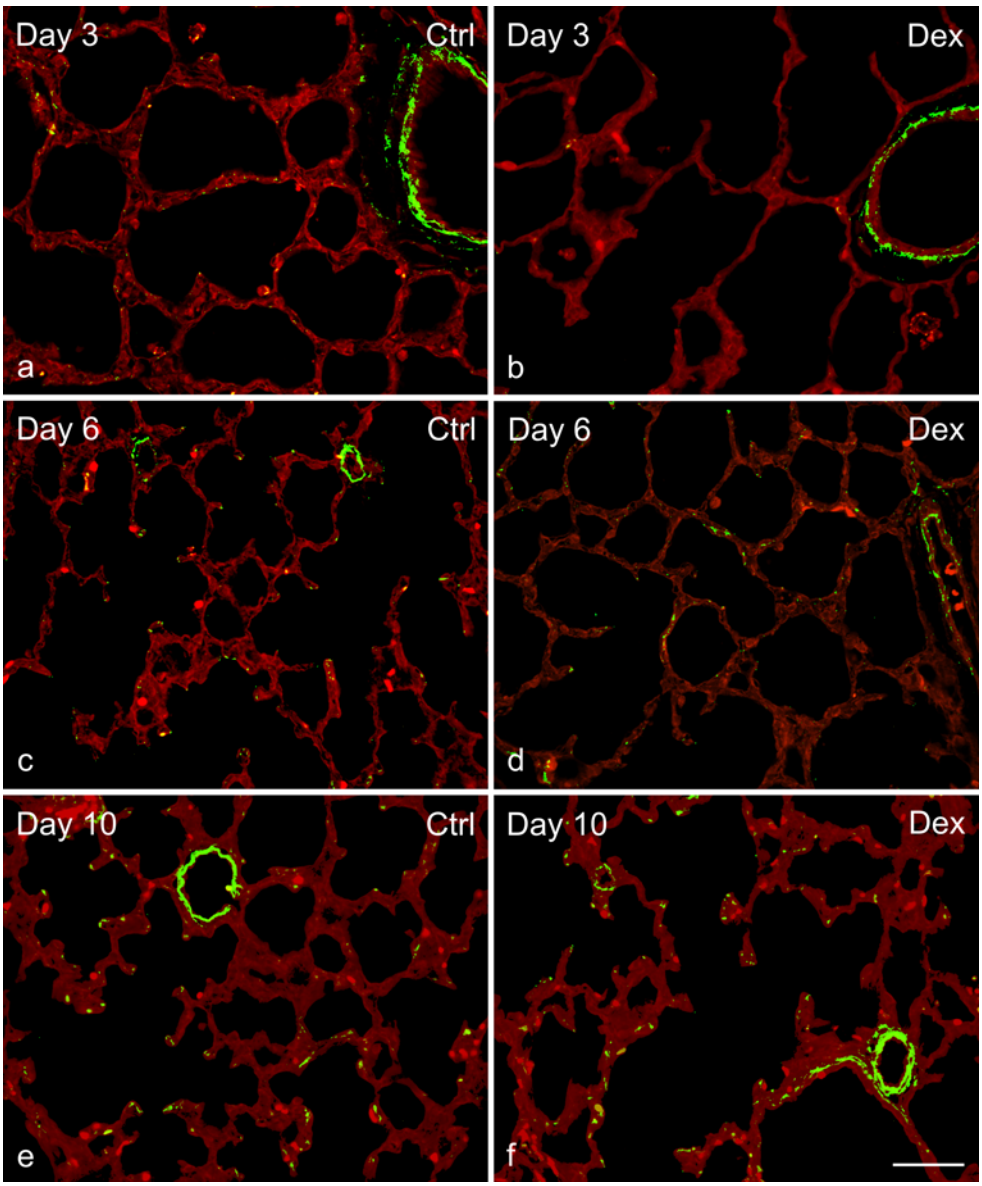

Fig. 4 Elastin localization during rat lung development. The expression of elastin is shown by *green immunofluorescence* between postnatal days P3 and P10. In alveolar septa of CTRL (**a**, **c**, **e**), elastin was present on P3. Its expression increased strongly during the period studied. In alveolar septa of Dex-treated animals (**b**, **d**, **f**), only small amounts of elastin were observed before P6. Later, no difference was detected anymore (**e**, **f**). Unspecific red fluorescence was used to visualize the lung tissue. *Bar* 20 μm

between embryonic days E13 and E18) and a second one during early alveolarization. Thereafter, its expression decreases to almost non-measurable values (Young et al. 1994). TNC is specifically located at the epithelial–mesenchymal interface at sites of airway branching during morphogenesis of the airways and at the tips of the growing alveolar septa during early alveolarization (Kaarteenaho-Wiik et al. 2001; Young et al. 1994; Zhao and Young 1995). Reduction in TNC function by addition of TNC antiserum to lung explants inhibited the branching process (Young et al. 1994). We have recently shown that branching morphogenesis was dramatically hampered in TNC knockout mice (Roth-Kleiner et al. 2004). In analogy, we hypothesized that the delaying effect of Dex on early alveolarization might be due to a down-regulation of TNC expression. In fact, Dex has been shown to decrease TNC gene expression in different cell lines including human lung fibroblasts (Degen et al. 2009; Jagodzinski et al. 2004). We found a transient reduction in TNC gene expression on P4 and a delayed and decreased appearance of TNC protein in lungs of Dex-treated rat pups. Additionally, elastin expression within the lung parenchyma was delayed. We therefore suspect that the delayed formation of alveolar septa observed in the Dex-treated lungs

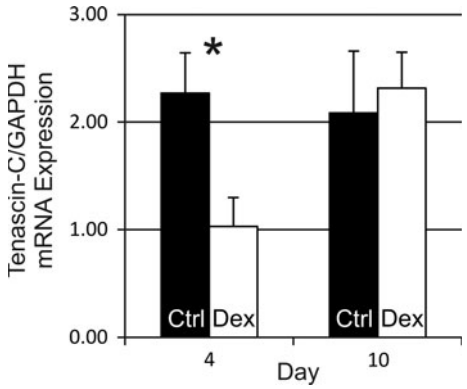

Fig. 5 Tenascin-C (TNC) gene expression in rat lung tissue. TNC gene expression was quantified by qRT-PCR in lung tissue on postnatal day P4 and P10 comparing CTRL (*black bars*) and Dex-treated newborn rats (*white bars*). $N = 3$–5 per group. $^*P < 0.05$

might, at least in part, be due to a temporarily suppressed and delayed expression of ECM proteins. Interestingly, both sites of specific TNC expression during lung development are especially exposed to mechanical strain. During branching, these forces are provoked by fetal breathing movements (Schittny et al. 2000) and during alveolarization by the centripetal uplifting of the growing secondary septa (Schittny et al. 2008). Taking into account that TNC expression has been shown to be up-regulated by mechanical strain, we might suspect that the specific spatial and temporal distribution pattern of TNC during lung development is, at least in part, coordinated by mechanical stimuli (Chiquet et al. 2004; Yamamoto et al. 1999). The importance of mechanical strain in alveolar formation is highlighted by the fact, that apart from TNC, other mechano-sensing structures like elastin and myofibroblasts are essential for the subdivision of the sacculi by newly formed septa. Accumulation of PDGF-A and PDGF-A-receptor-α expressing myofibroblasts is essential for septal growth (Bostrom et al. 1996, 2002; Lindahl et al. 1997). These cells have been shown to produce elastin (McGowan et al. 2008). Massaro et al. have already shown in the 1980s that subcutaneous injections of Dex between P4 and P13 impaired saccule septation, hampered alveolar surface increase, and reduced specifically the volume density of lipid-ladened fibroblasts; however, the mechanisms remained unknown (Massaro and Massaro 1986; Massaro et al. 1985). Our results suggest that the presence of TNC, elastin, and the myofibroblasts seems to be required to uplift secondary septa. We therefore suggest that the combined presence of myofibroblasts, TNC, and elastin is a prerequisite for early or classical alveolarization.

Recently, an increasing body of evidence has emerged showing that beside the current model of classical alveolarization and microvascular maturation followed by isometric lung growth, there has to be a second phase of alveolar formation (Hyde et al. 2007; Mund et al. 2008; Narayanan et al. 2012; Schittny et al. 2008). This late alveolarization seems to be distinctly different from classical alveolarization. Whereas the latter mechanism is dependent on a preexisting double capillary layer, of which one capillary layer will be included in the uplifted newly formed septum, late alveolarization happens after microvascular maturation, i.e., the fusion of the double layer into one. Most likely, a local duplication of the single-layered capillary network at the base of the newly forming septa takes place (Schittny et al. 2008). Furthermore, late alveolarization seems to be independent of TNC expression at the free septal edges, as its expression vanishes in rats at this site after P14. The exact molecular mechanisms involved in late alveolarization remains to be elucidated.

Most likely due to a prolonged expression of TNC, we did not find any difference of lung structure complexity anymore in Dex-treated animals compared to CTRL by P21. Indeed, we even found an accelerated septal formation during late alveolarization on day P36. Whether this compensatory catch-up septal formation in Dex-treated animals represents an acceleration of the physiological late alveolarization or a regenerative process after early Dex treatment might be a semantic question. However, these results demonstrate that Dex-administration during the saccular stage has a profound effect on lung development, although the resulting lung structure in adulthood seems to be unaltered. Whether all these structural changes during lung development have an impact on lung function would be very interesting to investigate, but was out of the scope of this study. In recent years, there has been increasing evidence that alveolarization and vascular formation are connected. We and others have recently shown that Dex interferes with vascular formation by decreasing VEGF-R2 and by accelerating microvascular maturation (Massaro and Massaro 2004; Roth-Kleiner et al. 2005). Therefore, we focused in this study on the investigation of structural elements involved in the formation of the airspaces.

In conclusion, even a short course of Dex-administration during the saccular stage of lung development delays the first phase of alveolarization (classical alveolarization). This delay includes the suppression of key elements necessary for alveolarization, i.e., the expression of TNC and elastin. Catch-up alveolar formation, however, is possible if steroid treatment is of short duration. It takes place in both phases of alveolarization: as an extended expression of TNC (first phase) and a higher rate of newly forming septa during second phase.

Acknowledgments This study was supported by the Swiss National Science Foundation grants 310000-109874, 310030-125397, and 310000-118238. We thank Mrs. Bettina de Breuyn and Mr. Christoph Lehmann for expert technical assistance and Dr. Amela Groso for her

help at the beamline. Thanks to Dr. M. Chiquet for providing the anti-TNC antibody.

References

Banks BA, Macones G, Cnaan A, Merrill JD, Ballard PL, Ballard RA (2002) Multiple courses of antenatal corticosteroids are associated with early severe lung disease in preterm neonates. J Perinatol 22:101–107

Blanco LN, Massaro GD, Massaro D (1989) Alveolar dimensions and number: developmental and hormonal regulation. Am J Physiol 257:L240–L247

Bostrom H, Willetts K, Pekny M, Leveen P, Lindahl P, Hedstrand H, Pekna M, Hellstrom M, Gebre-Medhin S, Schalling M, Nilsson M, Kurland S, Tornell J, Heath JK, Betsholtz C (1996) PDGF-A signaling is a critical event in lung alveolar myofibroblast development and alveogenesis. Cell 85:863–873

Bostrom H, Gritli-Linde A, Betsholtz C (2002) PDGF-A/PDGF alpha-receptor signaling is required for lung growth and the formation of alveoli but not for early lung branching morphogenesis. Dev Dyn 223:155–162

Burri PH (2006) Structural aspects of postnatal lung development—alveolar formation and growth. Biol Neonate 89:313–322

Chiquet M, Sarasa-Renedo A, Tunc-Civelek V (2004) Induction of tenascin-C by cyclic tensile strain versus growth factors: distinct contributions by Rho/ROCK and MAPK signaling pathways. Biochim Biophys Acta 1693:193–204

Corroyer S, Schittny JC, Djonov V, Burri PH, Clement A (2002) Impairment of rat postnatal lung alveolar development by glucocorticoids: involvement of the p21CIP1 and p27KIP1 cyclin-dependent kinase inhibitors. Pediatr Res 51:169–176

Degen M, Goulet S, Ferralli J, Roth M, Tamm M, Chiquet-Ehrismann R (2009) Opposite effect of fluticasone and salmeterol on fibronectin and tenascin-C expression in primary human lung fibroblasts. Clin Exp Allergy 39:688–699

Doyle LW, Ehrenkranz RA, Halliday HL (2010) Dexamethasone treatment after the first week of life for bronchopulmonary dysplasia in preterm infants: a systematic review. Neonatology 98:289–296

Eichenwald EC, Stark AR (2007) Are postnatal steroids ever justified to treat severe bronchopulmonary dysplasia? Arch Dis Child Fetal Neonatal Ed 92:F334–F337

Faber V, Quentin-Hoffmann E, Breuer B, Schittny J, Volker W, Kresse H (1992) Colocalization of a large heterodimeric proteoglycan with basement membrane proteins in cultured cells. Eur J Cell Biol 59:37–46

Grier DG, Halliday HL (2004) Effects of glucocorticoids on fetal and neonatal lung development. Treat Respir Med 3:295–306

Haberthur D, Hintermuller C, Marone F, Schittny JC, Stampanoni M (2010) Radiation dose optimized lateral expansion of the field of view in synchrotron radiation X-ray tomographic microscopy. J Synchrotron Radiat 17:590–599

Halliday HL (2004) Use of steroids in the perinatal period. Paediatr Respir Rev 5((suppl A)):S321–S327

Halliday HL (2011) Postnatal steroids: the way forward. Arch Dis Child Fetal Neonatal Ed 96:F158–F159

Howard CV, Reed MG (2005) Three dimensional measurement in microscopy Unbiased stereology. BIOS Scientific Publishers, Oxon, pp 143–145

Hsia CC, Hyde DM, Ochs M, Weibel ER (2010) How to measure lung structure–what for? On the "standards for the quantitative assessment of lung structure". Respir Physiol Neurobiol 171:72–74

Hyde DM, Blozis SA, Avdalovic MV, Putney LF, Dettorre R, Quesenberry NJ, Singh P, Tyler NK (2007) Alveoli increase in number but not size from birth to adulthood in rhesus monkeys. Am J Physiol Lung Cell Mol Physiol 293:L570–L579

Jagodzinski M, Drescher M, Zeichen J, Hankemeier S, Krettek C, Bosch U, van Griensven M (2004) Effects of cyclic longitudinal mechanical strain and dexamethasone on osteogenic differentiation of human bone marrow stromal cells. Eur Cell Mater 7:35–41

Kaarteenaho-Wiik R, Kinnula V, Herva R, Pääkkö P, Pöllänen R, Soini Y (2001) Distribution and mRNA expression of tenascin-C in developing human lung. Am J Respir Cell Mol Biol 25:341–346

Liggins GC, Howie RN (1972) A controlled trial of antepartum glucocorticoid treatment for prevention of the respiratory distress syndrome in premature infants. Pediatrics 50:515–525

Lindahl P, Karlsson L, Hellstrom M, Gebre-Medhin S, Willetts K, Heath JK, Betsholtz C (1997) Alveogenesis failure in PDGF-A-deficient mice is coupled to lack of distal spreading of alveolar smooth muscle cell progenitors during lung development. Development 124:3943–3953

Luyet C, Burri PH, Schittny JC (2002) Suppression of cell proliferation and programed cell death by dexamethasone during postnatal lung development. Am J Physiol Lung Cell Mol Physiol 282:477–483

Massaro D, Massaro GD (1986) Dexamethasone accelerates postnatal alveolar wall thinning and alters wall composition. Am J Physiol 251:R218–R224

Massaro D, Massaro GD (2004) Critical period for alveologenesis and early determinants of adult pulmonary disease. Am J Physiol Lung Cell Mol Physiol 287:L715–L717

Massaro D, Teich N, Maxwell S, Massaro GD, Whitney P (1985) Postnatal development of alveoli. Regulation and evidence for a critical period in rats. J Clin Investig 76:1297–1305

McGowan SE, Grossmann RE, Kimani PW, Holmes AJ (2008) Platelet-derived growth factor receptor-alpha-expressing cells localize to the alveolar entry ring and have characteristics of myofibroblasts during pulmonary alveolar septal formation. Anat Rec (Hoboken) 291:1649–1661

Mund SI, Stampanoni M, Schittny JC (2008) Developmental alveolarization of the mouse lung. Dev Dyn 237:2108–2116

Narayanan M, Owers-Bradley J, Beardsmore CS, Mada M, Ball I, Garipov R, Panesar KS, Kuehni CE, Spycher BD, Williams SE, Silverman M (2012) Alveolarization continues during childhood and adolescence: new evidence from helium-3 magnetic resonance. Am J Respir Crit Care Med 185:186–191

Roth-Kleiner M, Hirsch E, Schittny JC (2004) Fetal lungs of tenascin-C-deficient mice grow well, but branch poorly in organ culture. Am J Respir Cell Mol Biol 30:360–366

Roth-Kleiner M, Berger TM, Tarek MR, Burri PH, Schittny JC (2005) Neonatal dexamethasone induces premature microvascular maturation of the alveolar capillary network. Dev Dyn 233: 1261–1271

Scherle W (1970) A simple method for volumetry of organs in quantitative stereology. Mikroskopie 26:57–60

Schittny JC, Kresse H, Burri PH (1995) Immunostaining of a heterodimeric dermatan sulphate proteoglycan is correlated with smooth muscles and some basement membranes. Histochem Cell Biol 103:271–279

Schittny JC, Paulsson M, Vallan C, Burri PH, Kedei N, Aeschlimann D (1997) Protein cross-linking mediated by tissue transglutaminase correlates with the maturation of extracellular matrices during lung development. Am J Respir Cell Mol Biol 17:334–343

Schittny JC, Djonov V, Fine A, Burri PH (1998) Programmed cell death contributes to postnatal lung development. Am J Respir Cell Mol Biol 18:786–793

Schittny JC, Miserocchi G, Sparrow MP (2000) Spontaneous peristaltic airway contractions propel lung liquid through the bronchial tree of intact and fetal lung explants. Am J Respir Cell Mol Biol 23:11–18

Schittny JC, Mund SI, Stampanoni M (2008) Evidence and structural mechanism for late lung alveolarization. Am J Physiol Lung Cell Mol Physiol 294:L246–L254

Schwyter M, Burri PH, Tschanz SA (2003) Geometric properties of the lung parenchyma after postnatal glucocorticoid treatment in rats. Biol Neonate 83:57–64

Trummer-Menzi E, Gremlich S, Schittny JC, Denervaud V, Stampanoni M, Post M, Gerber S, Roth-Kleiner M (2012) Evolution of gene expression changes in newborn rats after mechanical ventilation with reversible intubation. Pediatr Pulmonol 47:1204–1214

Tschanz SA, Damke BM, Burri PH (1995) Influence of postnatally administered glucocorticoids on rat lung growth. Biol Neonate 68:229–245

Tschanz SA, Makanya AN, Haenni B, Burri PH (2003) Effects of neonatal high-dose short-term glucocorticoid treatment on the lung: a morphologic and morphometric study in the rat. Pediatr Res 53:72–80

Yamamoto K, Dang QN, Kennedy SP, Osathanondh R, Kelly RA, Lee RT (1999) Induction of tenascin-C in cardiac myocytes by mechanical deformation. Role of reactive oxygen species. J Biol Chem 274:21840–21846

Young SL, Chang LY, Erickson HP (1994) Tenascin-C in rat lung: distribution, ontogeny and role in branching morphogenesis. Dev Biol 161:615–625

Zhao Y, Young SL (1995) Tenascin in rat lung development: in situ localization and cellular sources. Am J Physiol 269:L482–L491